Adaptive Nonlinear Control of a pH Neutralization Process

Michael A. Henson, *Member, IEEE,* and Dale E. Seborg

***Abstract*—An adaptive nonlinear control strategy for a bench-scale pH neutralization system is developed and experimentally evaluated. The pH process exhibits severe nonlinear and time-varying behavior and therefore cannot be adequately controlled with a conventional PI controller. The nonlinear controller design is based on a modified input–output linearization approach which accounts for the implicit output equation in the reaction invariant model. Because the reaction invariants cannot be measured on-line and the linearized system is unobservable, a nonlinear output feedback controller is developed by combining the input–output linearizing controller with a reduced-order, open-loop observer. The adaptive nonlinear control strategy is obtained by augmenting the non-adaptive controller with an indirect parameter estimation scheme which accounts for unmeasured buffering changes. Experimental tests demonstrate the superior performance of the adaptive nonlinear controller as compared to a non-adaptive nonlinear controller and conventional PI controller.**

I. Introduction

THE CONTROL of pH is common in the chemical process and biotechnological industries. For instance, the pH of effluent streams from wastewater treatment plants must be maintained within stringent environmental limits [1], [2]. Tight control of pH is also critical in the production of pharmaceuticals [3]. However, high performance and robust pH control is often difficult to achieve due to nonlinear and time-varying process characteristics. These processes can exhibit severe static nonlinear behavior because the process gain can vary several orders of magnitude over a modest range of pH values. Moreover, the titration curve may be time varying due to unmeasured changes in the buffering capacity.

As a result of these characteristics, several adaptive nonlinear control strategies [4]–[10] have been proposed for pH neutralization processes. However, these pH control techniques suffer from one or more of the following shortcomings: (i) a process model with linear dynamics is employed; (ii) process nonlinearities are incompletely compensated; (iii) slowly time varying behavior is assumed; (iv) the control actions are generated using iterative calculations which may not converge; and (v) the approach is evaluated using an unbuffered pH system which does not account for the time-varying nature of industrial processes. Hence, most pH control techniques do not adequately address the nonlinear and time-varying characteristics of pH processes. In this paper, a new adaptive nonlinear control strategy which addresses these shortcomings is developed.

In a previous paper [11], we developed adaptive, nonlinear control strategies for a bench-scale pH neutralization process. The nonlinear controller was designed by applying input–output linearization theory to a reaction invariant model of the system [4], [12]. Although reaction invariants usually cannot be measured on-line, they were assumed to be available for feedback control. Because the model exhibits significant nonlinear and time-varying behavior, a conventional PI controller and non-adaptive version of the nonlinear controller yield unacceptable performance. Three adaptive nonlinear controllers were developed by combining the input–output linearizing controller with nonlinear parameter estimators which account for unmeasured buffering changes. The direct approach of Sastry and Isidori [13] was shown to have poor setpoint tracking characteristics and high sensitivity to sampling. The indirect technique of Teel *et al.* [14] provides excellent performance but cannot be employed if the reaction invariants are unmeasured. A new indirect adaptive control approach was proposed which provides outstanding setpoint tracking and disturbance rejection. Moreover, the new method is suitable for experimental application where the reaction invariants cannot be measured and sampling is required.

In this paper, an implementable version of the indirect adaptive nonlinear control strategy proposed by Henson and Seborg [11] is developed and experimentally evaluated. As in the previous study, the adaptive nonlinear controller is designed by combining an input–output linearizing controller with a new indirect parameter estimator. Because the system is unobservable, an implementable controller is obtained by augmenting the state feedback controller with a reduced-order, open-loop observer which provide on-line estimates of the reaction invariants. Non-adaptive and adaptive versions of the nonlinear output feedback controller are compared to a conventional PI controller using a bench-scale pH neutralization system at UCSB [15].

II. The Reaction Invariant Model

A simplified schematic diagram of the UCSB bench-scale pH neutralization system is shown in Fig. 1. The process consists of an acid stream (q_1), buffer stream (q_2) and base stream (q_3) that are mixed in tank 1. Prior to mixing, the acid stream enters tank 2 which introduces additional flow dynamics. The acid and base flow rates are regulated with flow control valves, while the buffer flow rate is controlled

Manuscript received September 28, 1993; revised May 23, 1994. Paper recommended by Associate Editor B. Egardt.

M. A. Henson was with the Department of Chemical Engineering, University of California, Santa Barbara. He is now with the Department of Chemical Engineering, Louisiana State University, Baton Rouge, LA, 70803-7303 USA.

D. E. Seborg is with the Department of Chemical Engineering, University of California, Santa Barbara, CA, 93106 USA.

IEEE Log Number 9403525.

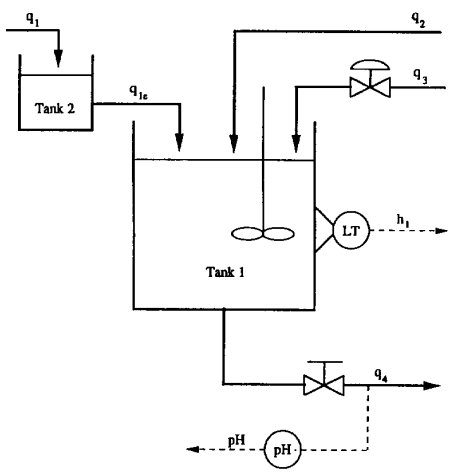

Fig. 1. The UCSB pH neutralization system.

manually with a rotameter. The tank level (h) and effluent pH (pH) are measured variables. Because the pH probe is located downstream from tank 1, a time delay (θ) is introduced in the pH measurement. Dilute acid and base streams are employed for safety and environmental reasons. The process is interfaced to an IBM PC/AT personal computer that is used for process monitoring and control. In this study, the pH is controlled by manipulating the base flow rate, and the acid and buffer flow rates are considered to be unmeasured disturbances. In the adaptive nonlinear control strategy presented in Section III, the buffer flow rate is estimated from input–output data. More detailed descriptions of the process and the computer control system are presented elsewhere [15], [16].

The dynamic model of the pH neutralization system shown in Fig. 1 is derived using conservation equations and equilibrium relations. The model also includes valve and transmitter dynamics as well as hydraulic relationships for the tank outlet flows. Modeling assumptions include perfect mixing, constant density, and complete solubility of the ions involved. The model is presented briefly below; more detailed derivations are available elsewhere [15], [16].

The chemical reactions for the system are:

$$H_2CO_3 \leftrightarrow HCO_3^- + H^+ \quad (1)$$

$$HCO_3^- \leftrightarrow CO_3^{=} + H^+ \quad (2)$$

$$H_2O \leftrightarrow OH^- + H^+. \quad (3)$$

The corresponding equilibrium constants are:

$$K_{a1} = \frac{[HCO_3^-][H^+]}{[H_2CO_3]} \quad (4)$$

$$K_{a2} = \frac{[CO_3^{=}][H^+]}{[HCO_3^-]} \quad (5)$$

$$K_w = [H^+][OH^-]. \quad (6)$$

The chemical equilibria is modeled by defining two reaction invariants [4], [12] for each inlet stream ($i \in [1, 4]$):

$$W_{ai} = [H^+]_i - [OH^-]_i - [HCO_3^-]_i - 2[CO_3^{=}]_i \quad (7)$$

$$W_{bi} = [H_2CO_3]_i + [HCO_3^-]_i + [CO_3^{=}]_i. \quad (8)$$

The invariant W_a is a charge related quantity, while W_b represents the concentration of the $CO_3^{=}$ ion. Unlike pH, these invariants are conserved quantities. The pH can be determined from W_a and W_b using the following relations [16]:

$$W_b \frac{\frac{K_{a1}}{[H^+]} + \frac{2K_{a1}K_{a2}}{[H^+]^2}}{1 + \frac{K_{a1}}{[H^+]} + \frac{K_{a1}K_{a2}}{[H^+]^2}} + W_a + \frac{K_w}{[H^+]} - [H^+] = 0 \quad (9)$$

$$pH = -\log([H^+]). \quad (10)$$

The dynamic model of the neutralization process is developed as follows. A mass balance on tank 2 yields,

$$A_2 \frac{dh_2}{dt} = q_1 - q_{1e} \quad (11)$$

where h_2 and A_2 are the level and cross-sectional area of tank 2, respectively. The exit flow rate q_{1e} is modeled with the following flow-head relation,

$$q_{1e} = C_{v1} h_2^{0.5} \quad (12)$$

where C_{v1} is a constant valve coefficient. An overall mass balance on tank 1 yields,

$$A_1 \frac{dh_1}{dt} = q_{1e} + q_2 + q_3 - q_4 \quad (13)$$

where A_1 is the cross-sectional area of tank 1. The exit flow rate q_4 is modeled as,

$$q_4 = C_{v4}(h_1 + z)^n \quad (14)$$

where C_{v4} is a constant valve coefficient, n is a constant valve exponent, and z is the vertical distance between the bottom of tank 1 and the outlet for q_4. By combining mass balances on each of the ionic species in the system, the following differential equations for the effluent reaction invariants (W_{a4}, W_{b4}) can be derived [16]:

$$A_1 h_1 \frac{dW_{a4}}{dt} = q_{1e}(W_{a1} - W_{a4}) + q_2(W_{a2} - W_{a4}) + q_3(W_{a3} - W_{a4}) \quad (15)$$

$$A_1 h_1 \frac{dW_{b4}}{dt} = q_{1e}(W_{b1} - W_{b4}) + q_2(W_{b2} - W_{b4}) + q_3(W_{b3} - W_{b4}). \quad (16)$$

The pH and level transmitters are modeled as first order transfer functions with unity gain and time constants τ_{pH} and τ_h, respectively. The desired flow rates q_1 and q_3 serve as setpoints for cascade flow control loops with sampling period $\Delta t_c = 1$ s which are modeled as first-order transfer functions with unity gain and time constant τ_v. The sampling period for pH measurement and control is $\Delta t = 15$ s. Nominal model parameters and operating conditions are given in Table I.

III. Adaptive Nonlinear Controller Design

In this section, an adaptive nonlinear control strategy for the UCSB pH neutralization system is described and simulation results are presented. As demonstrated by Henson [17] and the experimental results in Section IV, a conventional PI controller must be tuned very conservatively to maintain stability for high gain conditions and very sluggish control is

TABLE I
NOMINAL OPERATING CONDITIONS FOR THE PH SYSTEM

$[q_1]$ = 0.003 M HNO_3	q_1 = 16.6 ml/s
$[q_2]$ = 0.03 M $NaHCO_3$	q_2 = 0.55 ml/s
$[q_3]$ = 0.003 M NaOH,	q_3 = 15.6 ml/s
0.0005 M $NaHCO_3$	q_{1c} = 16.6 ml/s
A_1 = 207 cm^2	q_4 = 32.8 ml/s
A_2 = 42 cm^2	$W_{a1} = 3.00 \times 10^{-3}$ M
z = 11.5 cm	W_{b1} = 0 M
n = 0.607	$W_{a2} = -0.03$ M
$K_{a1} = 4.47 \times 10^{-7}$	W_{b2} = 0.03 M
$K_{a2} = 5.62 \times 10^{-11}$	$W_{a3} = -3.05 \times 10^{-3}$ M
$K_w = 1.00 \times 10^{-14}$	$W_{b3} = 5.00 \times 10^{-5}$ M
Δt = 15.0 s	h_1 = 14.0 cm
Δt_c = 1.0 s	h_2 = 3.0 cm
τ_{pH} = 15.0 s	$W_{a4} = 4.32 \times 10^{-4}$ M
τ_h = 15.0 s	$W_{b4} = 5.28 \times 10^{-4}$ M
τ_v = 6.0 s	pH = 7.0
θ = 10.0 s	

therefore obtained for other operating regimes. Although the non-adaptive nonlinear controller presented accounts for the nonlinear static behavior, it does not explicitly address time-varying process behavior caused by unmeasured buffering changes. Superior performance for buffering variations is obtained by treating the buffer flow rate as a unknown, time-varying parameter which is updated with a recursive least-squares algorithm. Experimental results for the non-adaptive and adaptive nonlinear controllers are presented in Section IV.

A. Non-Adaptive Nonlinear Control

The nonlinear controller design is based on a slightly simplified version of the simulation model described in Section II. In particular, the dynamics of the pH and level transmitters and the flow dynamics of tank 2 are neglected. With these simplifications, a nonlinear state-space model of the process can be obtained by defining the state variables, disturbance, input, and output as,

$$x \triangleq [W_{a4}\ W_{b4}\ h_1]^T, d \triangleq q_2, \quad u_a \triangleq q_3, y \triangleq \text{pH} \tag{17}$$

where u_a is the actual value of the base flow rate which differs from the base flow rate calculated by the controller (u_c) due to the valve dynamics. Using these definitions, the process model has the form,

$$\dot{x} = f(x) + g(x)u_a + p(x)d \tag{18}$$

$$c(x, y) = 0 \tag{19}$$

where

$$f(x) = \left[\frac{q_1}{A_1 x_3}(W_{a1} - x_1)\ \frac{q_1}{A_1 x_3}(W_{b1} - x_2)\ \frac{1}{A_1}(q_1 - C_{v4}(h_1 + z)^n)\right]^T \tag{20}$$

$$g(x) = \left[\frac{1}{A_1 x_3}(W_{a3} - x_1)\ \frac{1}{A_1 x_3}(W_{b3} - x_2)\ \frac{1}{A_1}\right]^T \tag{21}$$

$$p(x) = \left[\frac{1}{A_1 x_3}(W_{a2} - x_1)\ \frac{1}{A_1 x_3}(W_{b2} - x_2)\ \frac{1}{A_1}\right]^T \tag{22}$$

$$c(x, y) = x_1 + 10^{y-14} - 10^{-y} + x_2 \frac{1 + 2 \times 10^{y-pK_2}}{1 + 10^{pK_1 - y} + 10^{y-pK_2}}. \tag{23}$$

The valve dynamics are modeled by a first-order differential equation with unity gain and time constant τ_v:

$$\dot{u}_a = -\frac{1}{\tau_v}u_a + \frac{1}{\tau_v}u_c. \tag{24}$$

The nonlinear controller design is based on a modified input–output linearization approach [11] which accounts for the implicit output equation in (23). Taking the time derivative of (23) using (18) and rearranging yields,

$$\dot{y} = -c_y^{-1}(x, y)c_x(y)[f(x) + g(x)u_a + p(x)d] \tag{25}$$

where ((26) and (27) are at the bottom of the page.)

Because $c_y^{-1}(x, y)c_x(y)g(x) \neq 0$ for all x and y of interest, the model has relative degree $r = 1$ and standard input–output linearization techniques [18], [19] can be applied to (25). The nonlinear controller is designed by solving the following equation for u_a:

$$-c_y^{-1}(x, y)c_x(y)[f(x) + g(x)u_a + p(x)d] = v. \tag{28}$$

The "new" input v is chosen as,

$$v = -2\varepsilon^{-1}y + \varepsilon^{-2}\int_0^t (y_{sp} - y)d\tau \tag{29}$$

where y_{sp} is the pH setpoint. Hence, the input–output linearizing controller can be written as ((30) at the bottom of the next page) where $0 < \varepsilon < \infty$ is the controller tuning parameter. If there is no plant/model mismatch, (30) yields the following closed-loop transfer function (CLTF):

$$\frac{y(s)}{y_{sp}(s)} = \frac{1}{(\varepsilon s + 1)^2}. \tag{31}$$

The parameter $\varepsilon = 1$ min is chosen to provide a compromise between performance and robustness to modeling errors. This value of ε is approximately one-half the time constant for the open-loop responses shown in Section IV.

$$c_x(y) = \left[1\ \frac{1 + 2 \times 10^{y-pK_2}}{1 + 10^{pK_1 - y} + 10^{y-pK_2}}\ 0\right]^T \tag{26}$$

$$c_y(x, y) = (\ln 10)\left[10^{y-14} + 10^{-y} + x_2 \frac{10^{pK_1 - y} + 10^{y-pK_2} + 4\{10^{pK_1 - y}\}\{10^{y-pK_2}\}}{\{1 + 10^{pK_1 - y} + 10^{y-pK_2}\}^2}\right]. \tag{27}$$

In the experimental system, the pH (y) and tank 1 level (x_3) are measured but the reaction invariants (x_1 and x_2) must be estimated. Below we show that it is not possible to design a closed-loop observer because the pH process model is unobservable. Local nonlinear observability can be analyzed by determining the rank of a matrix that is the nonlinear generalization of the observability matrix used in linear system theory [18]. However, this approach requires the computation of a set of Lie derivatives that are very complicated for the pH neutralization model. Because linear observability is obviously a necessary condition for nonlinear observability, a linearized model can be used for initial observability analysis. If the linear model is unobservable, a nonlinear closed-loop observer does not exist and there is no reason to proceed with the nonlinear analysis.

For the pH model, the linearized model at any operating point can be expressed as,

$$\dot{x}' = \begin{bmatrix} a_{11} & 0 & a_{13} \\ 0 & a_{22} & a_{23} \\ 0 & 0 & a_{33} \end{bmatrix} x' + \begin{bmatrix} b_1 \\ b_2 \\ b_3 \end{bmatrix} u' = Ax' + bu' \tag{32}$$

$$y' = [c_1 \quad c_2 \quad 0]x' = cx' \tag{33}$$

where

$$a_{11} = a_{22} = -\frac{1}{A\bar{x}_3}(\bar{q}_1 + \bar{d} + \bar{u}). \tag{34}$$

In (32)–(34) the prime ($'$) and bar ($\bar{\ }$) superscripts represent deviation and steady-state values, respectively. A simple calculation shows that the linear observability matrix has the form,

$$\begin{bmatrix} c \\ cA \\ cA^2 \end{bmatrix} = \begin{bmatrix} c_1 & c_2 & 0 \\ c_1 a_{11} & c_2 a_{22} & 0 \\ c_1 a_{11}^2 & c_2 a_{22}^2 & * \end{bmatrix} \tag{35}$$

where the asterisk (*) represents a non-zero entry. Because $a_{11} = a_{22}$, the first two rows of the observability matrix are linearly dependent and the linearized system is unobservable at every operating point. The unobservability is due to the decoupled nature of the reaction invariant differential equations in (15) and (16).

Because the linearized pH model contains an unobservable mode, a nonlinear closed-loop observer does not exist. However, an open-loop observer can be used to generate estimates of the reaction invariants without the assumption of observability. Using this approach, errors in the initial conditions of the state variables will decay according to the dynamics of the process instead of a rate specified in the observer design. In order to facilitate experimental implementation, the observer design is based on a discretized version of the process model. Because the differential equations for the reaction invariants are decoupled, the invariants can be estimated sequentially. Invariant W_{b4} can be estimated with an open-loop observer, and then an estimate of W_{a4} can be generated from the estimated W_{b4} and the measured pH, using the output equation. Hence, the reaction invariants are estimated with a reduced-order, open-loop observer. A related estimation scheme has been proposed by Girardot [20].

The open-loop observer for W_{b4} is obtained by discretizing the differential equation for W_{b4} in (18) using a semi-implicit Euler scheme,

$$\hat{x}_{2,k} = \frac{\Gamma_{k-1}}{\Psi_{k-1}} \tag{36}$$

where

$$\Gamma_{k-1} \triangleq \hat{x}_{2,k-1} + \Delta t/(A_1 x_{3,k-1}) \times (q_1 W_{a1} + W_{a3} u_{a,k-1} + W_{a2} d_{k-1}) \tag{37}$$

$$\Psi_{k-1} \triangleq 1 + \Delta t/(A_1 x_{3,k-1}) \times (q_1 + u_{a,k-1} + d_{k-1}). \tag{38}$$

In (36)–(38), $\Delta t = 15$ s is the sampling period, z_k represents the value of variable z at sampling instant k, and the carat superscript ($\hat{\ }$) represents a predicted value. The estimate of W_{a4} can be generated by solving the output equation in (23) for W_{a4} using the estimated value of W_{b4} and the measured pH:

$$\hat{x}_{1,k} = -10^{y_k - 14} + 10^{-y_k} - \hat{x}_{2,k} \times \frac{1 + 2 \times 10^{y_k - pK_2}}{1 + 10^{pK_1 - y_k} + 10^{y_k - pK_2}}. \tag{39}$$

In order to compensate for the dynamics of the base flow control valve, the differential equation in (24) is discretized using an implicit Euler scheme to yield:

$$u_{a,k} = \frac{1}{1 + \frac{\Delta t}{\tau_v}} \left\{ u_{a,k-1} + \frac{\Delta t}{\tau_v} u_{c,k-1} \right\} \tag{40}$$

The estimate of the last implemented base flow rate, $u_{a,k-1}$, can then be employed in the control law to provide compensation for the valve dynamics. The non-adaptive nonlinear output feedback control law is derived by discretizing (30) using the estimated values of the reaction invariants,

$$\begin{aligned} \gamma(\hat{x}_k, y_k) u_{c,k} = {} & \gamma(\hat{x}_{k-1}, y_{k-1}) u_{a,k-1} + \varepsilon^{-2} \Delta t (y_{\text{sp}} - y_k) \\ & - 2\varepsilon^{-1}(y_k - y_{k-1}) + \alpha(\hat{x}_k, y_k) \\ & - \alpha(\hat{x}_{k-1}, y_{k-1}) + \beta(\hat{x}_k, y_k) d_k \\ & - \beta(\hat{x}_{k-1}, y_{k-1}) d_{k-1} \end{aligned} \tag{41}$$

where

$$\alpha(\hat{x}_k, y_k) \triangleq c_y^{-1}(\hat{x}_k, y_k) c_x(y_k) f(\hat{x}_k) \tag{42}$$

$$\beta(\hat{x}_k, y_k) \triangleq c_y^{-1}(\hat{x}_k, y_k) c_x(y_k) p(\hat{x}_k) \tag{43}$$

$$\gamma(\hat{x}_k, y_k) \triangleq -c_y^{-1}(\hat{x}_k, y_k) c_x(y_k) g(\hat{x}_k). \tag{44}$$

$$u_a = \frac{\varepsilon^{-2} \int_0^t (y_{\text{sp}} - y) d\tau - 2\varepsilon^{-1} y + c_y^{-1}(x, y) c_x(y) [f(x) + p(x) d]}{-c_y^{-1}(x, y) c_x(y) g(x)} \tag{30}$$

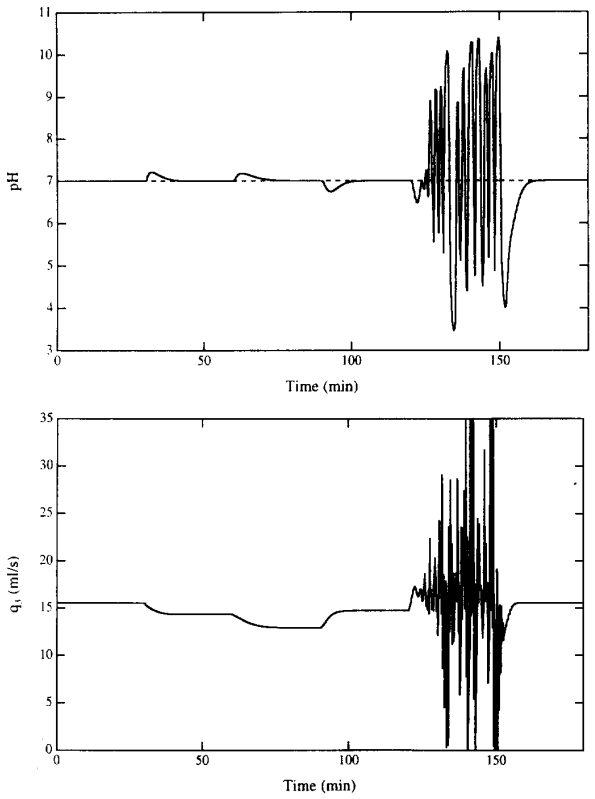

Fig. 2. Simulated non-adaptive nonlinear control for buffer flow rate disturbances.

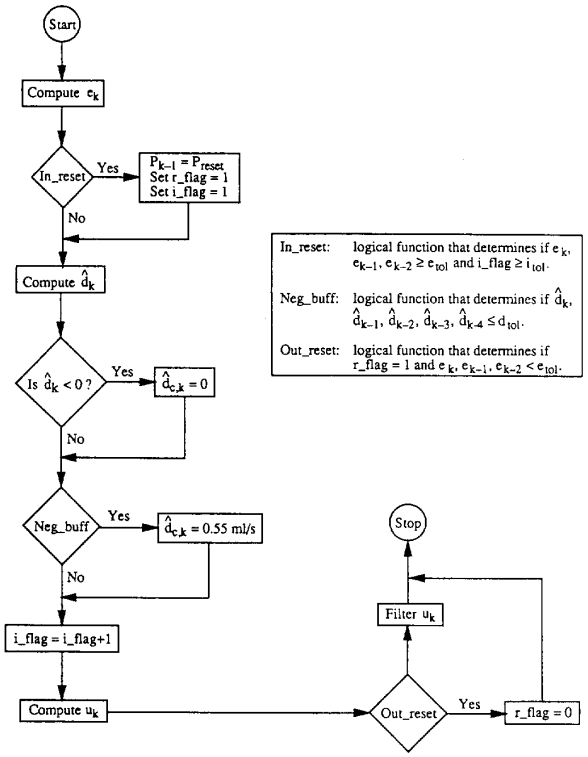

Fig. 3. Flow diagram for the adaptive nonlinear controller.

In the non-adaptive case the nominal buffer flow rate $d = 0.55$ ml/s is used in the control law. The controller is initialized with the values of the reaction invariants shown in Table I.

In the simulation study [17], the non-adaptive nonlinear controller provides vastly superior setpoint tracking and improved performance for unmeasured disturbances in the acid flow rate as compared to a conventional PI controller. However, the simulation results in Fig. 2 demonstrate that the non-adaptive controller provides poor control for the sequence of buffer flow rate changes shown in Table II. For the first three disturbances, the pH responses are somewhat sluggish but still superior to PI controller responses [17]. However, when $q_2 \rightarrow 0$ ml/s the closed-loop system is unstable because of the large increase in the process gain. The estimates of the reaction invariants are particularly poor in this case [17]. As long as the actual value of W_{b4} remains sufficiently large, the controller can overcome the poor estimates. However, when the buffer flow rate is changed to zero, $W_{b4} \rightarrow 0$ and the controller cannot stabilize the system. As shown in the next section, significantly improved estimates of W_{b4} can be obtained by combining the output feedback controller with a parameter estimator that estimates the buffer flow rate.

TABLE II
STANDARD BUFFER AND ACID FLOW RATE DISTURBANCES

Time (min)	q_2 (ml/s)	q_1 (ml/s)
0	0.55	16.6
30	1.2	14.6
60	2.0	18.6
90	1.0	16.6
120	0	–
150	0.55	–

B. Parameter Estimation

In this section, the nonlinear output feedback controller is combined with a parameter estimator which provides on-line estimates of the unmeasured buffer flow rate. Henson and Seborg [11] have investigated via simulation the performance of three buffer flow rate estimation schemes assuming the reaction invariants are available for feedback. The direct approach of Sastry and Isidori [13] and the indirect scheme of Teel *et al.* [14] are shown to be unsuitable for the experimental system where the reaction invariants cannot be measured and sampling is required. Conversely, a new indirect adaptive control technique was developed which provides excellent performance and is suitable for actual implementation. The proposed estimation scheme is based on a recursive least-squares algorithm with covariance resetting. The modification of the parameter estimator for output feedback is presented below.

The buffer flow rate estimator is derived by discretizing the expression for the time derivative of y in (25). A forward difference discretization is employed to preserve linear

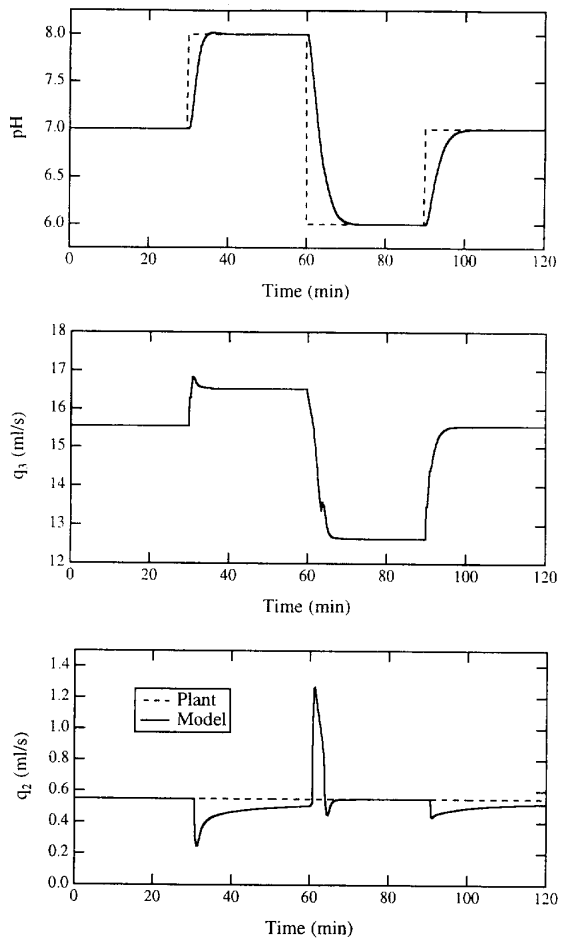

Fig. 4. Simulated adaptive nonlinear control for setpoint changes.

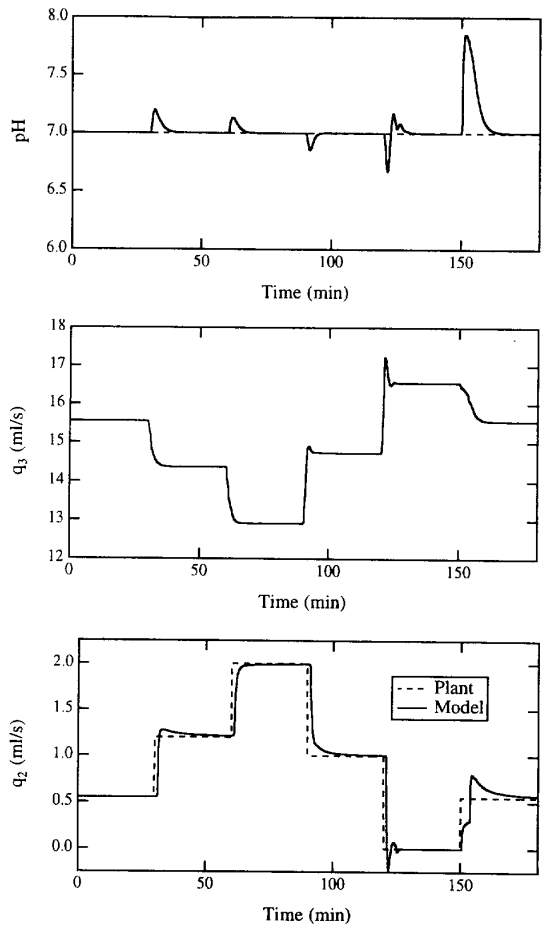

Fig. 5. Simulated adaptive nonlinear control for buffer flow rate disturbances.

parameterization. The resulting expression is:

$$y_k = y_{k-1} - \Delta t c_y^{-1}(x_{k-1}, y_{k-1}) c_x(x_{k-1}) \times [f(x_{k-1}) + g(x_{k-1}) u_{a,k-1} + p(x_{k-1}) d_{k-1}]. \quad (45)$$

The estimation equation follows directly from (45) with two modifications. First, the unmeasured state variables (x_1 and x_2) are replaced by their estimates ($\hat{x}_1$ and $\hat{x}_2$) obtained from the open-loop observer in (36)–(39). Second, a filtered pH value (y^f) is used instead of the measured pH (y) in order to reduce undesirable covariance resetting due to process noise present in the experimental system. A discrete-time, first-order transfer function with unity gain and time constant α_e is employed for pH measurement filtering. With these modifications, the estimation error is calculated as,

$$e_k = \nu_k - \eta_k \hat{d}_{k-1} \quad (46)$$

where

$$\nu_k \triangleq \Delta t c_y^{-1}(\hat{x}_{k-1}, y_{k-1}^f) c_x(\hat{x}_{k-1}) \times [f(\hat{x}_{k-1}) + g(\hat{x}_{k-1}) u_{a,k-1}] + y_k^f - y_{k-1}^f \quad (47)$$

$$\eta_k \triangleq -\Delta t c_y^{-1}(\hat{x}_{k-1}, y_{k-1}^f) c_x(\hat{x}_{k-1}) p(\hat{x}_{k-1}). \quad (48)$$

The estimated buffer flow rate ($\hat{d}_k$) is updated using a normalized least-squares estimator [21]:

$$\hat{d}_k = \hat{d}_{k-1} + \frac{P_{k-2}\eta_k e_k}{1 + P_{k-2}\eta_k^2} \quad (49)$$

$$P_{k-1} = P_{k-2} - \frac{P_{k-2}^2 \eta_k^2}{1 + P_{k-2}\eta_k^2}. \quad (50)$$

In the state feedback case [11], the adaptive nonlinear controller provides excellent tracking and regulatory performance using a simple covariance resetting scheme. However, these results were obtained assuming that the reaction invariants are available for feedback, the liquid level is constant, and the dynamics of the actuators and transmitters are insignificant. The increased complexity of the present case necessitates a considerably more elaborate scheme to ensure satisfactory interactions between the estimator and the controller. The specific modifications employed are discussed below.

1. The covariance is reset only when three consecutive values of the prediction error exceed an error tolerance e_{tol} [20], [22]. Hence, the covariance resetting algorithm is $P(0) = P(k_r) = P_{\text{reset}}$ where $k_r =$

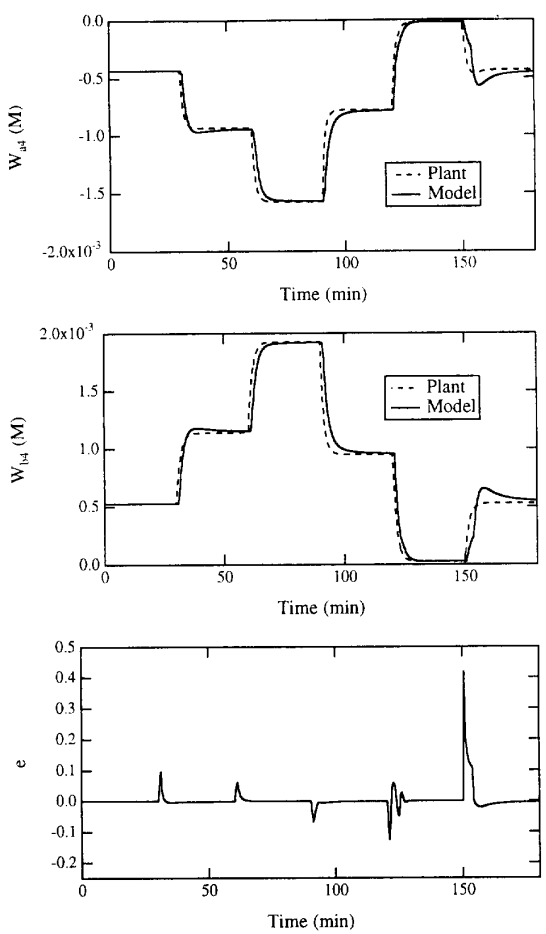

Fig. 6. Simulated adaptive nonlinear control for buffer flow rate disturbances.

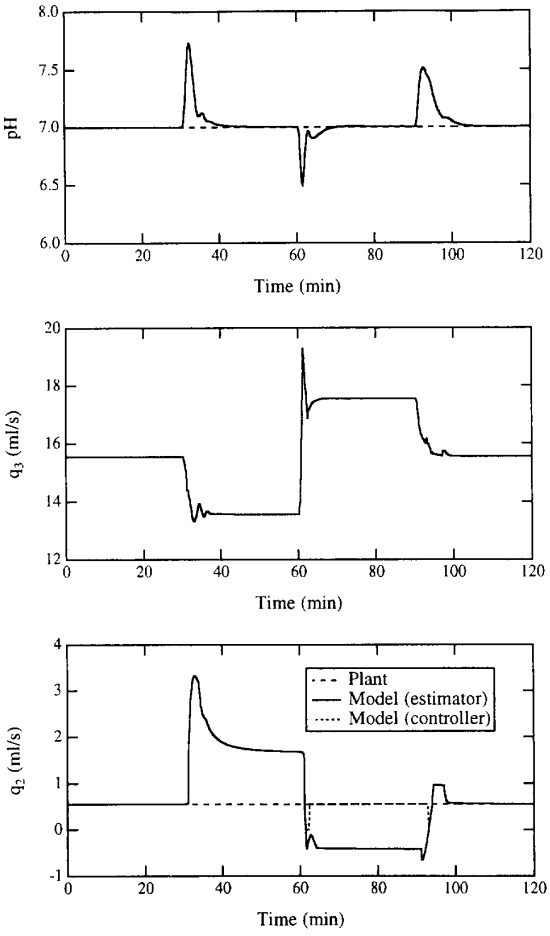

Fig. 7. Simulated adaptive nonlinear control for acid flow rate disturbances.

$\{k \mid |e_k|, |e_{k-1}|, |e_{k-2}| \geq e_{\text{tol}}\}$. This modification and the pH measurement filtering described previously help reduce undesirable covariance resetting due to process noise.

2. An upper limit on the frequency of covariance resets is enforced. The frequency is determined by a tuning parameter i_{tol} which represents the minimum number of sampling periods between covariance resets. This modification is necessitated by the extremely fast decay of the covariance under most operating conditions.
3. Different values of the estimated buffer flow rate and reaction invariants are maintained for the estimator and controller. Under most conditions the estimated buffer flow rates are the same. However, the estimated buffer flow rate used by the controller ($\hat{d}_{c,k}$) is restricted to be non-negative and is set to the nominal value in Table I (0.55 ml/s) if five consecutive values produced by the estimator are less than a tolerance d_{tol}. The estimated reaction invariants used by the controller are then computed as in (36)–(39) except that $\hat{d}_{c,k}$ is used instead of $\hat{d}_k$. Restricting $\hat{d}_{c,k}$ to be non-negative improves stability when the actual buffer flow rate drops to zero, while resetting $\hat{d}_{c,k}$ to the nominal value provides significantly improved performance for certain acid flow rate disturbances which cause a sustained negative value of $\hat{d}_k$.
4. Once the covariance is reset, the controller output is filtered until three consecutive values of the prediction error are less than a tolerance e_{tol}. The controller output is filtered using a discrete-time, first-order transfer function with unity gain and time constant α_c. This modification improves stability when the actual buffer flow rate drops to zero.

The adaptive nonlinear output feedback control algorithm is summarized in Fig. 3. Nominal estimator and controller tuning parameters are shown in Table III. For all simulations, the state and parameter estimator are initialized with the reaction invariants and buffer flow rate in Table I.

The simulated setpoint tracking performance of the adaptive nonlinear controller is shown in Fig. 4. The adaptive controller provides good, but slightly asymmetrical, setpoint responses and very reasonable control moves. Note that the controller provides good setpoint tracking despite generating poor transient estimates of the buffer flow rate (q_2). This behavior,

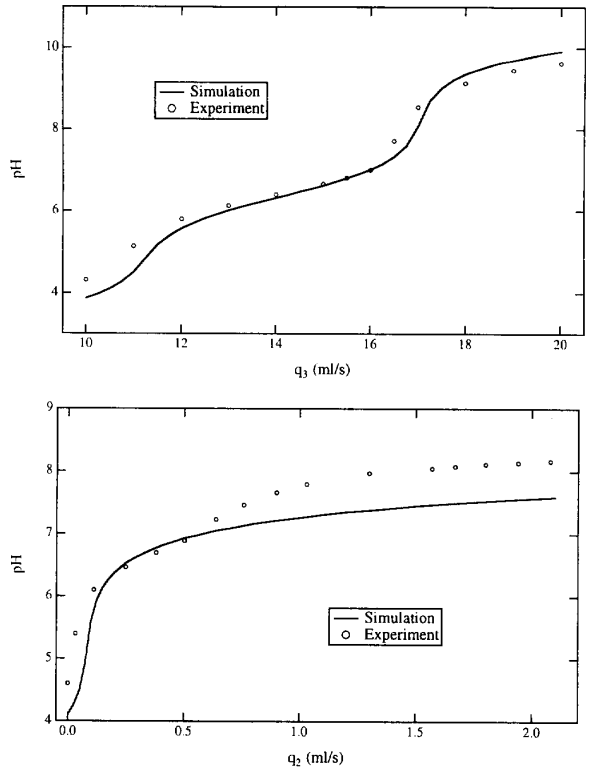

Fig. 8. Simulated and experimental titration curves for q_3 (top) and q_2 (bottom) changes.

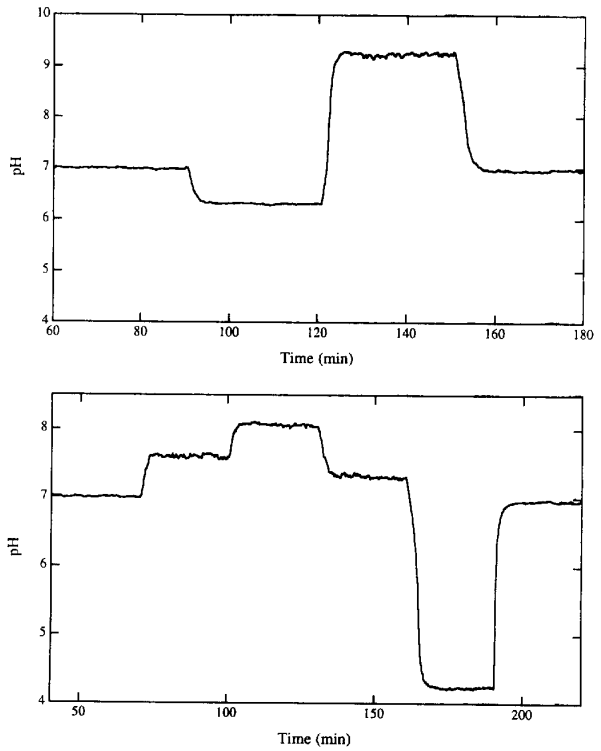

Fig. 9. Open-loop responses for base (top) and buffer (bottom) flow rate changes.

TABLE III
NOMINAL TUNING PARAMETERS FOR THE ADAPTIVE NONLINEAR CONTROLLER

P_{reset}	100
e_{tol}	0.035
i_{tol}	12
α_e	0.472
α_c	0.472
d_{tol}	−0.1 ml/s
ε	1 min

which is not present in the state feedback case [11], can be attributed to sampling. The model discretization introduces modeling error which causes the estimator to enter covariance reset and modify the estimated q_2 after each setpoint change. After the initial transient, however, the estimated q_2 returns to a value which is sufficiently close to the true value (0.55 ml/s) to yield good performance.

The simulated performance of the adaptive nonlinear controller for the buffer flow rate disturbances in Table II is shown in Figs. 5 and 6. The adaptive controller clearly outperforms the non-adaptive controller in Fig. 2 for the critical buffer flow rate change $q_2 \rightarrow 0$ ml/s at $t = 120$ min. The adaptive controller also provides slightly improved control for the other q_2 disturbances, and generates reasonable control moves. The parameter estimator tracks q_2 very effectively, especially when $q_2 \rightarrow 0$ ml/s. The estimated reaction invariants and the prediction error are shown in Fig. 6. Like the buffer flow rate, excellent estimation of the reaction invariants is obtained for all q_2 changes. Note that the estimation error is quickly returned to zero after each q_2 change, and that the largest estimation errors are obtained for the final two disturbances which correspond to the most significant buffering changes.

In Fig. 7 the simulated performance of the adaptive controller for the acid flow rate changes in Table II is shown. Because the state estimator uses a constant value of the acid flow rate to produce the reaction invariant estimates, acid flow rate disturbances represent a robustness test for the adaptive controller. The controller provides significantly improved pH responses as compared to the non-adaptive controller [17]. The control moves of the adaptive controller are reasonable, but a rather large overshoot is obtained for the second disturbance. Because all modeling errors are attributed to buffering changes, the adaptive controller yields poor estimates of the buffer flow rate. Note that the estimated q_2 used by the controller $\hat{d}_{c,k}$) is reset to the nominal value of 0.55 ml/s after the second disturbance as previously discussed. Because the estimated q_2 is poor, the state estimator generates inaccurate estimates of the reaction invariants [17]. Despite the poor parameter and state estimates, the adaptive controller provides satisfactory control. Because the acid flow rate disturbances have a significant effect on the prediction error [17], the performance of the parameter estimator cannot be improved by increasing the prediction error tolerance without significantly degrading closed-loop performance for q_2 disturbances.

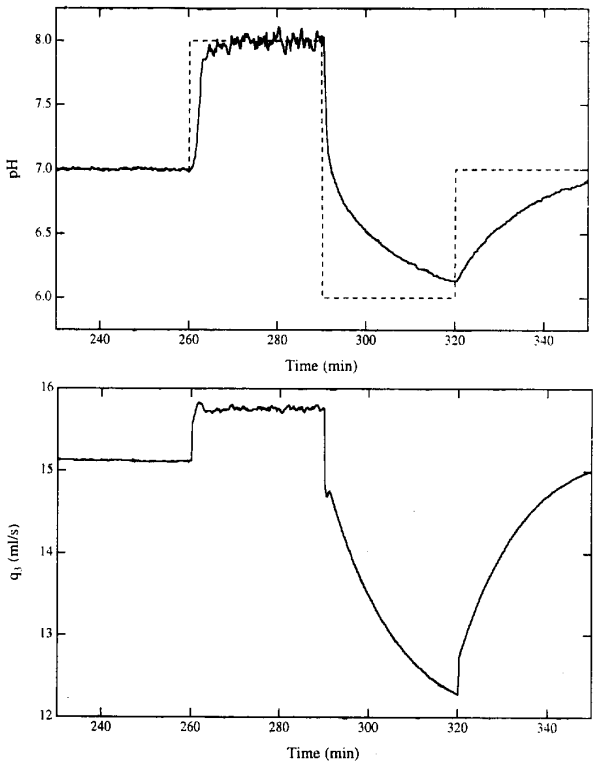

Fig. 10. PI control for setpoint changes.

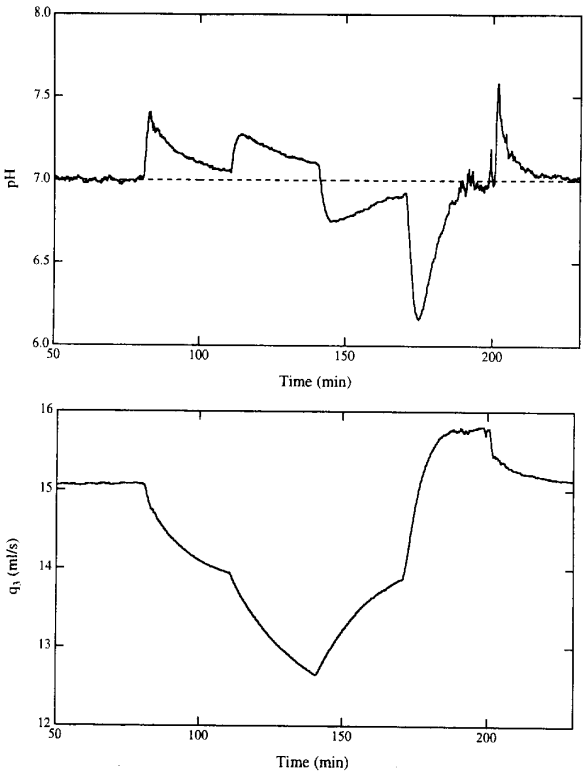

Fig. 11. PI control for modified buffer flow rate disturbances.

IV. Experimental Results

In this section, the adaptive nonlinear output feedback controller presented in Section III is applied to the UCSB pH neutralization system. In order to ascertain the advantages offered by the adaptive nonlinear control strategy, experimental results are also presented for a conventional PI controller and the non-adaptive version of the nonlinear controller. The controllers are evaluated for setpoint changes and unmeasured disturbances in the buffer and acid flow rates.

A. Open-Loop Behavior

In this section, the steady-state and dynamic open-loop behavior of the experimental pH system is investigated. Simulated and experimental titration curves for base and buffer flow rate changes are shown in Fig. 8. For the base flow rate changes, the experimental titration curve matches that obtained via simulation reasonably well over a wide range of pH values. The most significant deviations occur at low and high pH values which should not be encountered in closed-loop operation if the controller is performing adequately. However, the differences in the titration curves in the pH range 7–8 are important because this region will obviously be encountered. In this case, a slight overshoot in the pH response is expected because the model underestimates the process gain.

Conversely, the simulated and experimental titration curves are significantly different for buffer flow rate changes. The largest deviations occur at higher buffer flow rates where the experimental pH is significantly higher than predicted by simulation. The results demonstrate that the pH deviations are not simply (e.g. linearly) related to the buffer flow rate. A variety of tests were conducted to locate the cause of the discrepancy, but a plausible explanation of the results was not obtained. All attempts to reduce this plant/model mismatch by adjusting model parameters increased the mismatch at lower buffer flow rates. Because the pH deviations are relatively small for the more critical lower buffer flow rates, no adjustment of model parameters was attempted in any of the subsequent experiments. As shown below, the adaptive nonlinear controller is able to handle this modeling error.

Open-loop responses for the base and buffer flow rate changes indicated in Table II are shown in Fig. 9. Note that for all the experimental tests, the actual run time is plotted and, therefore, the plots do not begin with $t = 0$. However, the input changes used in Fig. 9 are identical to those listed in Table II with the starting time of the experimental run simply taken as an offset. The pH responses for the base changes are very similar to those obtain via simulation [17]. However, the experimental and simulated pH responses for buffer flow rate changes are significantly different for buffer flow rates higher than the nominal value of 0.55 ml/s. Based on the titration curve in Fig. 8, this behavior is expected.

B. PI Control

In this section, the performance of a conventional PI controller is evaluated for setpoint changes and unmeasured

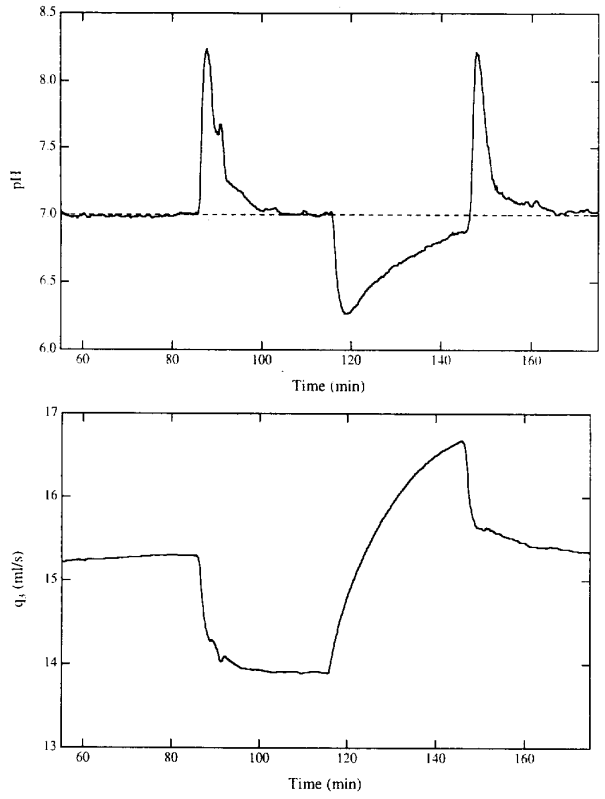

Fig. 12. PI control for modified acid flow rate disturbances.

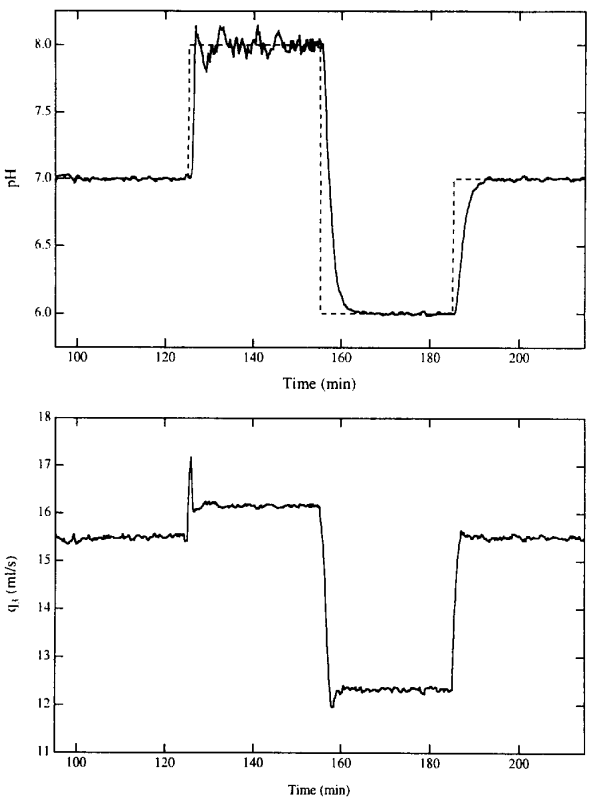

Fig. 13. Non-adaptive nonlinear control for setpoint changes.

TABLE IV
MODIFIED BUFFER AND ACID FLOW RATE DISTURBANCES

Time (min)	q_2 (ml/s)	q_1 (ml/s)
0	0.55	16.6
30	1.2	15.1
60	2.0	18.1
90	1.0	16.6
120	0.2	–
150	0.55	–

disturbances. Derivative action is not included in the controller because of the pH measurement time delay [20]. The controller tuning parameters ($K_c = 2.4$ ml/s, $\tau_I = 100$ s) employed are the same as those used in simulation studies [17]. The setpoint tracking behavior of the PI controller is shown in Fig. 10. The first setpoint change is tracked reasonably well, but the pH responses for the other two changes are extremely sluggish. The pH responses and manipulated input moves are very similar to those obtained in simulation [17]. The only significant differences between the two results is the process noise in the experimental system at the pH = 8 setpoint. The effects of process noise at this setpoint are much greater than in the other regions due to the magnitude of the process gain.

The performance of the PI controller for the modified sequence of buffer flow rate disturbances listed in Table IV is shown in Fig. 11. The standard disturbance sequence in Table II was modified because the PI controller was unable to handle the change where $q_2 \rightarrow 0$ ml/s. Because similar results were obtained for the nonlinear controllers and the disturbance is extremely severe, the controllers were evaluated for the more realistic changes in Table IV. In this case, at $t = 120$ min (170 min in Fig. 11) the buffer flow rate is changed to 0.2 ml/s instead of 0 ml/s. The pH responses in Fig. 11 are very sluggish for all the buffer flow rate disturbances and similar to those obtained via simulation [17]. Because of the larger process gains at lower buffer flow rates the controller has difficulty maintaining the pH at the setpoint after $q_2 \rightarrow 0.2$ ml/s. Note that due to plant/model mismatch, a steady-state value of the base flow rate slightly less than 15.55 ml/s was required to obtain a pH of 7. Typically, the necessary steady-state base flow rate was in the range 15.1–15.5 ml/s.

PI control for the modified set of acid flow rate disturbances listed in Table IV is shown in Fig. 12. The modified acid disturbances were employed in all the closed-loop experimental runs because the tank 1 level exceeds the allowable limit for the positive acid flow rate change in Table II. The modified disturbances are identical to those in Table II except that the magnitude of each disturbance is 1.5 ml/s instead of 2.0 ml/s. As predicted by simulation [17], the PI controller is sluggish for the first and third disturbances and cannot even reach the setpoint after the second disturbance.

C. Non-Adaptive Nonlinear Control

In this section, the non-adaptive version of the nonlinear output feedback controller presented in Section III is evaluated

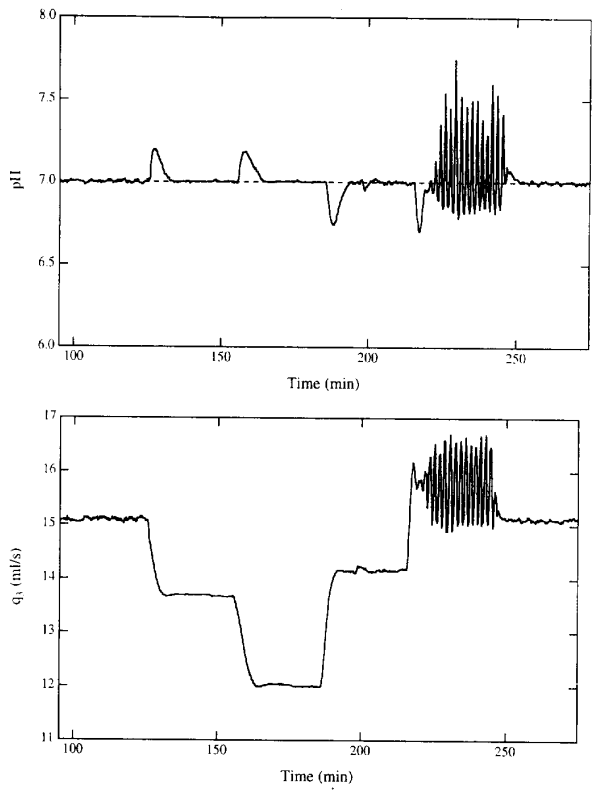

Fig. 14. Non-adaptive nonlinear control for modified buffer flow rate disturbances.

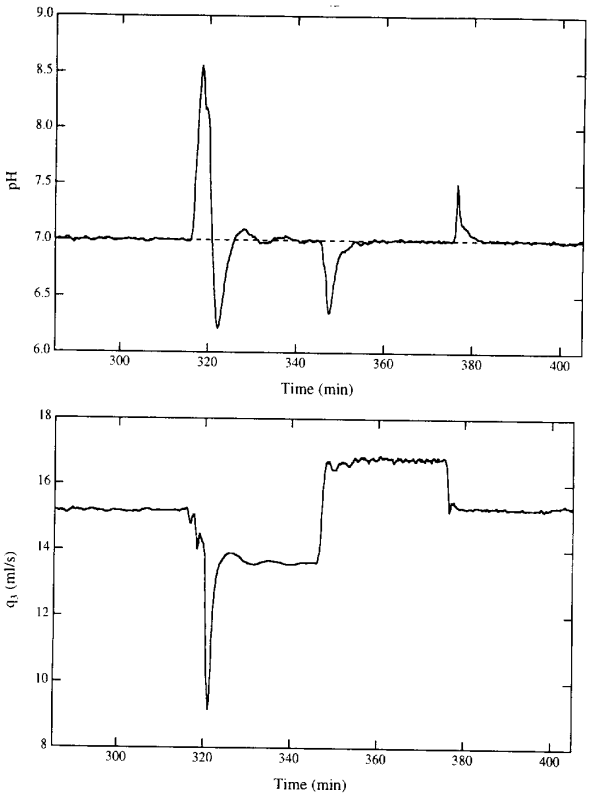

Fig. 15. Non-adaptive nonlinear control for modified acid flow rate disturbances.

for setpoint changes and unmeasured buffer and acid flow rate disturbances. For all the experimental runs, the controller was tuned with $\varepsilon = 1$ min and initialized with the values of the reaction invariants shown in Table I. The setpoint tracking performance of the non-adaptive controller is shown in Fig. 13. The controller tracks the second and third setpoint changes quickly and without overshoot, but has some difficulty maintaining the pH = 8 setpoint. The manipulated input moves demonstrate that the small pH oscillations at the pH = 8 setpoint are not due to the control moves, but rather result from noise that has a greater effect in this region because of the large process gain. For the second and third setpoint changes, the pH responses and control moves are very similar to those obtained by simulation [17].

Non-adaptive nonlinear control for the modified buffer flow rate disturbances in Table IV is shown in Fig. 14. As expected, the non-adaptive controller is able to reject most of the disturbances quite effectively. However, when $q_2 \rightarrow 0.2$ ml/s at $t = 215$ min, the controller produces oscillatory control moves which induce sustained pH oscillations. In fact, it appears that the oscillations result from a linear instability mechanism (i.e., the linearized closed-loop system is unstable at this operating point) because the pH and base flow rate are near their steady-state values when the oscillations begin. However, the non-adaptive controller provides excellent performance for this disturbance sequence in simulation [17]. The disparity between the simulation and experimental results when $9_2 \rightarrow 0.2$ ml/s is attributable to plant/model mismatch. Although the actual reaction invariants are not known in experiment, simulation results [17] indicate that the oscillatory behavior of the non-adaptive controller is due to poor estimates of the reaction invariants at low buffering. By using an estimate of the buffer flow rate to generate the reaction invariant estimates, the adaptive nonlinear controller should yield improved control.

The regulatory performance of the non-adaptive nonlinear controller for the modified acid flow rate disturbances in Table IV is shown in Fig. 15. Adequate pH control is obtained for the second and third disturbances. However, for the first disturbance the pH deviates from the setpoint by more than 1.5 pH units and then undershoots the setpoint by over 0.75 pH units. The poor pH response for this disturbance is caused by the controller twice moving the base flow rate in the wrong direction. Although smaller acid flow rate disturbances were used experimentally, this behavior is also predicted in simulation [17]. The poor regulatory performance of the non-adaptive controller is probably due to poor reaction invariant estimates. Because the nonlinear estimator uses a constant value of the acid flow rate to produce the reaction invariant estimates, it is not obvious that the adaptive nonlinear controller will provide improved performance in this case.

D. Adaptive Nonlinear Control

In this section, the adaptive nonlinear output feedback controller presented in Section III is evaluated for buffer and

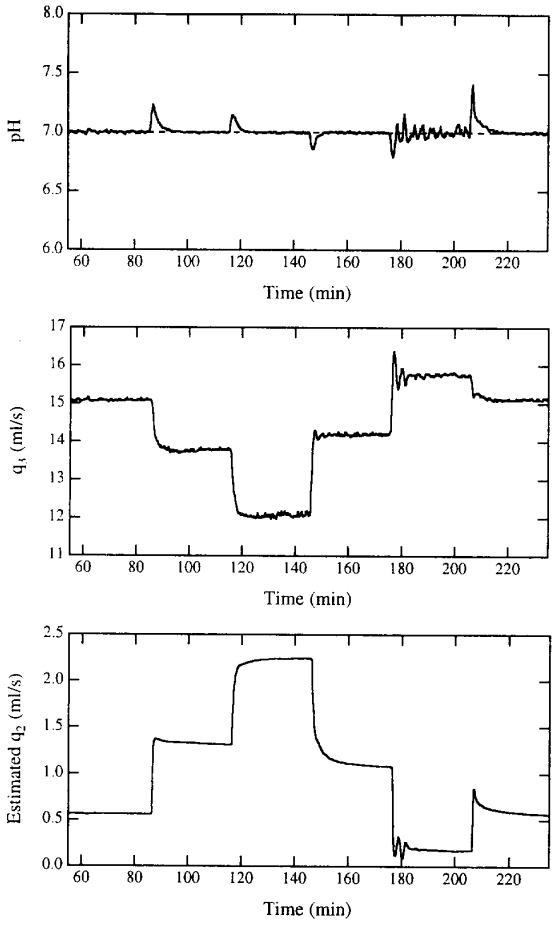

Fig. 16. Adaptive nonlinear control for modified buffer flow rate disturbances.

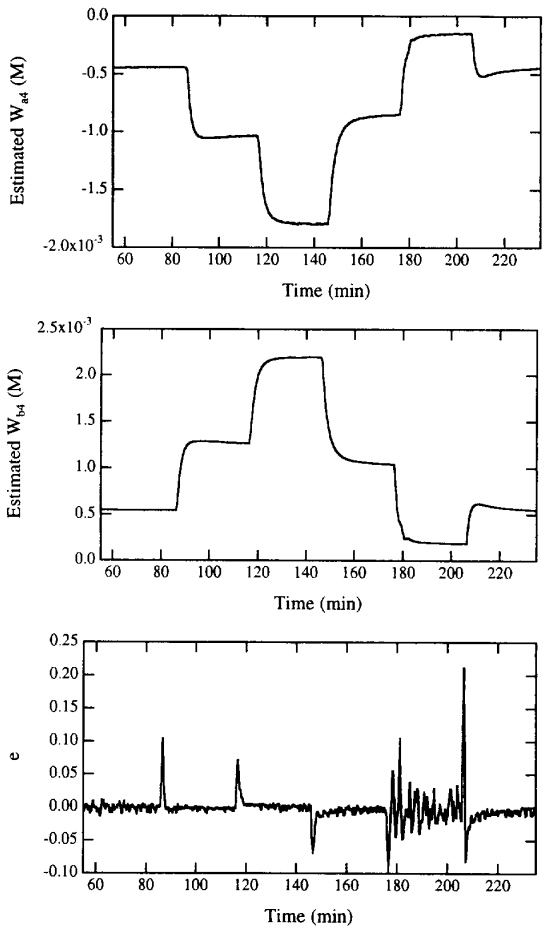

Fig. 17. Adaptive nonlinear control for modified buffer flow rate disturbances.

acid flow rate disturbances. The setpoint tracking performance of the adaptive controller was not investigated because Fig. 4 demonstrates that setpoint changes represent the least challenging test of the controller. Because excellent performance was obtained in simulation despite poor buffer flow rate and reaction invariant estimates, it is anticipated that the adaptive controller should yield good setpoint tracking in experiment. For all the experimental runs, the nonlinear adaptive controller was initialized with the nominal buffer flow rate and reaction invariants in Table I.

The regulatory performance of the adaptive nonlinear controller for the modified buffer flow rate disturbances in Table IV is shown in Figs. 16 and 17. As before, the controller was not evaluated for the standard buffer flow rate changes where $q_2 \rightarrow 0$ ml/s because of the effects of process noise in this high gain region. The controller and estimator tuning parameters in Table III are identical to those previously used for simulations. The pH responses in Fig. 16 demonstrate that the adaptive controller is able to provide excellent control for a wide range of buffering conditions. The adaptive controller clearly outperforms the PI controller shown in Fig. 11 for all the disturbances. Unlike the non-adaptive controller shown in Fig. 14, the adaptive controller is able to maintain the system at the setpoint when $q_2 \rightarrow 0.2$ ml/s. The small pH oscillations observed in the response of the adaptive controller for this disturbance are caused mainly by the high process gain and process noise. The adaptive controller yields slightly improved pH responses as compared to the non-adaptive controller for the other buffering disturbances. Fig. 16 also demonstrate that the improved performance provided by the adaptive controller is not due to large control moves. The pH responses and control moves observed experimentally are similar to the simulation results in Fig. 5 obtained using the standard buffer flow rate changes in Table II.

The estimated buffer flow rate produced by the adaptive nonlinear controller is also shown in Fig. 16. At near steady-state conditions, the estimation error is not more than 15% of the actual value. These errors are considerably less than those obtained under open-loop conditions [17]. The improved buffer flow rate estimation observed under closed-loop conditions is probably attributable to a more accurate model of the titration curve at a pH of 7. As shown in Fig. 8, the largest deviations in the q_2 and q_3 titration curves occur at pH values greater than 7. Hence, it appears that modeling errors

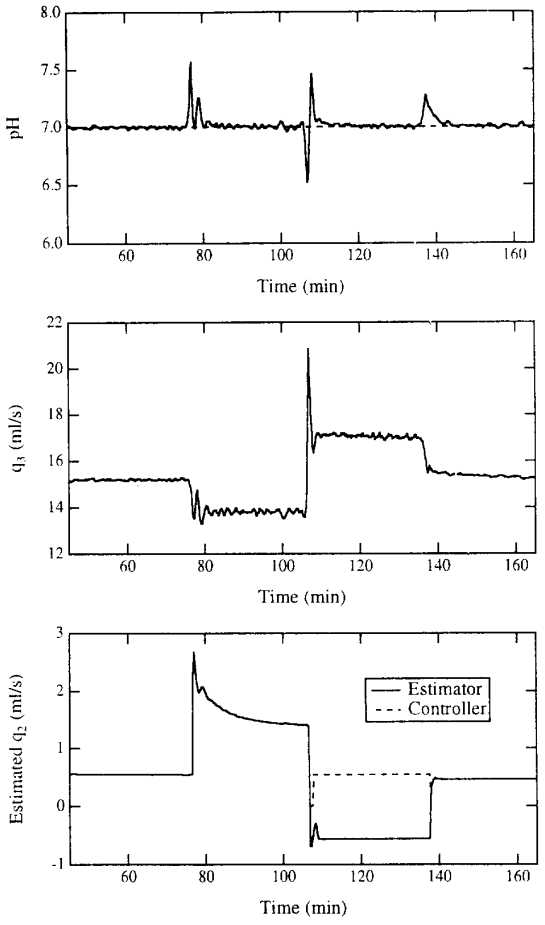

Fig. 18. Adaptive nonlinear control for modified acid flow rate disturbances.

in the titration curve are much less significant in closed-loop when the system is maintained near a pH of 7. Note that the buffer flow rates estimates obtained in simulation (Fig. 5) and experiment (Fig. 16) are very similar. The estimated reaction invariants and prediction error are shown in Fig. 17. Although the reaction invariants are not precisely known, the simulation results in Fig. 6 indicate that the nonlinear state estimator provides good tracking of the invariants. The prediction errors obtained in simulation (Fig. 6) and experiment (Fig. 17) are similar, although the effects of process noise are significant when $q_2 = 0.55$ ml/s.

The performance of the adaptive nonlinear controller for the modified acid flow rate disturbances in Table IV is shown in Fig. 18. As previously discussed, acid flow rate disturbances represent a robustness test because the adaptive controller is explicitly designed to account only for buffering changes. The pH responses in Fig. 18 demonstrate that the adaptive nonlinear controller provides superior control as compared to the PI controller in Fig. 12 and the non-adaptive nonlinear controller in Fig. 15. The most significant improvement occurs for the first disturbance where the PI and non-adaptive controllers allow large pH deviations from the setpoint and are quite sluggish. Conversely, the adaptive controller rejects this disturbance quickly without allowing large pH deviations. The control moves of the adaptive controller are considerably more aggressive than those of the PI controller but are comparable to those of the non-adaptive controller. The pH responses and control moves of the adaptive controller are similar to those obtained via simulation in Fig. 7 for the standard acid flow rate disturbances listed in Table 2.

The estimated buffer flow rates used by the nonlinear estimator and controller are also shown in Fig. 18. The results are similar to those in Fig. 7 obtained in simulation. In both cases, the estimated buffer flow rate used by the controller is poor. Note that after the second disturbance the buffer flow rate used by the controller is reset to the nominal value of 0.55 ml/s because the estimator generates a sustained buffer flow rate estimate that is less than the tolerance d_{tol} in Table III. Because a poor estimate of the buffer flow rate is generated, the reaction invariant estimates are also inaccurate [17]. Despite this poor estimation, adequate pH control is obtained.

V. Conclusion

An adaptive nonlinear output feedback control strategy for a pH neutralization process has been developed and experimentally evaluated. The adaptive nonlinear controller was developed by combining an input–output linearizing controller, an open-loop nonlinear state observer, and a recursive least squares parameter estimator. The input–output linearizing controller design accounts for the implicit output equation in the reaction invariant model. A reduced-order, open-loop state observer is employed because the reaction invariants cannot be measured and the process model is unobservable. The recursive least-squares estimator provides an estimate of the buffering capacity. Non-adaptive and adaptive versions of the nonlinear controller were compared to a conventional PI controller on a bench-scale pH neutralization system which exhibits significant nonlinear and time-varying behavior. Despite large plant/model mismatches, the non-adaptive nonlinear controller provides superior tracking and regulatory performance as compared to the PI controller for most conditions. However, if the buffering content of the system is sufficiently low, the non-adaptive controller exhibits unacceptable oscillatory behavior. Conversely, the adaptive nonlinear controller yields excellent control over a wide range of buffering conditions. The adaptive nonlinear controller also outperforms the PI and non-adaptive nonlinear controllers for unmeasured acid flow rate disturbances.

References

[1] F. G. Shinskey, *pH and pION Control in Process and Waste Streams.* New York: Wiley, 1973.
[2] G. K. McMillan, *pH Control.* Research Triangle Park, NC: Instrument Society of America, 1984.
[3] A. Johnson, "The control of fed-batch fermentation processes—A survey," *Automatica,* vol. 23, pp. 691–705, 1987.
[4] T. K. Gustafsson and K. V. Waller, "Dynamic modeling and reaction invariant control of pH," *Chem. Eng. Sci.,* vol. 38, pp. 389–398, 1983.

[5] ——, "Nonlinear and adaptive control of pH," *Ind. Eng. Chem. Res.*, vol. 31, pp. 2681–2693, 1992.
[6] P. Jutilia, "An application of adaptive pH-control algorithms based on physio-chemical modeling in a chemical waste-water treatment plant," *Int. J. Control*, vol. 38, pp. 639–655, 1983.
[7] G. A. Pajunen, "Comparison of linear and nonlinear adaptive control of pH-process," in *Proc. IEEE Conf. Decision and Control*, Ft. Lauderdale, FL, 1985, pp. 850–851.
[8] J. R. Parrish and C. B. Brosilow, "Nonlinear inferential control," *AIChE J.*, vol. 34, pp. 633–644, 1988.
[9] W. C. Li and L. T. Biegler, "Newton-type controllers for constrained nonlinear processes with uncertainty," *Ind. Eng. Chem. Res.*, vol. 29, pp. 1647–1657, 1990.
[10] G. L. Williams, R. R. Rhinehart, and J. B. Riggs, "In-line process-model-based control of wastewater pH using dual base injection," *Ind. Eng. Chem. Res.*, vol. 29, pp. 1254–1259, 1990.
[11] M. A. Henson and D. E. Seborg, "Nonlinear adaptive control of a pH neutralization process," in *Proc. IFAC DYCORD+92 Symp.*, College Park, MD, 1992, pp. 151–156.
[12] K. V. Waller and P. M. Makila, "Chemical reaction invariants and variants and their use in reactor modeling, simulation, and control," *Ind. Eng. Chem. Proc. Design and Develop.*, vol. 20, pp. 1 , 1981.
[13] S. S. Sastry and A. Isidori, "Adaptive control of linearizable systems," *IEEE Trans. Automatic Control*, vol. 34, pp. 1123–1131, 1989.
[14] A. Teel, R. Kadiyala, P. Kokotovic, and S. Sastry, "Indirect techniques for adaptive input–output linearization of non-linear systems," *Int. J. Control*, vol. 53, pp. 193–222, 1991.
[15] R. C. Hall and D. E. Seborg, "Modelling and self-tuning control of a multivariable pH neutralization process. Part I: Modelling and multiloop Control," in *Proc. Amer. Control Conf.*, Pittsburgh , PA, 1989, pp. 1822–1827.
[16] R. C. Hall, "Development of a multi-variable pH experiment," M. S. thesis, University of California, Santa Barbara, 1987.
[17] M. A. Henson, "Feedback linearization strategies for nonlinear process control," Ph. D. dissertation, University of California, Santa Barbara, 1992.
[18] A. Isidori, *Nonlinear Control Systems.* New York: Springer-Verlag, 1989.
[19] M. A. Henson and D. E. Seborg, "Critique of exact linearization strategies for process control," *J. Process Control*, vol. 1, pp. 122–139, 1991.
[20] D. M. Girardot, "Control of pH based on reaction invariants," M. S. thesis, University of California, Santa Barbara, 1989.
[21] G. C. Goodwin and K. S. Sin, *Adaptive Filtering Prediction and Control.* Englewood Cliffs, NJ: Prentice-Hall, 1984.
[22] S. Greenland, "An application of generalized predictive control to a nonlinear process," M. S. thesis, University of California, Santa Barbara, 1988.

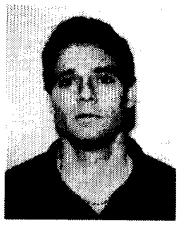

Michael A. Henson (S'90–M'92) received the B. S. degree from the University of Colorado (1985), M. S. degree from the University of Texas at Austin (1989), and the Ph. D. degree from the University of California, Santa Barbara (1992).

He is an Assistant Professor of Chemical Engineering at Louisiana State University. He has also held the position of Visiting Research Scientist with the DuPont Company. He has published 18 articles on process control and related topics. Along w ith Dr. D. E. Seborg, he is co-editor of the research monograph *Nonlinear Process Control* (Prentice-Hall). His principal research interests are: nonlinear process control and estimation; modeling and "reverse engineering" of biological control systems; and modeling, design, and control of membrane separation processes.

Dr. Henson is serving as an Associate Editor for the 1994 IEEE Conference on Decision and Control. He is a member of the AIChE.

Dale E. Seborg received the B. S. degree from the University of Wisconsin and the Ph. D. degree from Princeton University.

He is a Professor of Chemical Engineering at the University of California, Santa Barbara. Before joining UCSB in 1977, he taught at the University of Alberta for nine years. He served as department chairman at UCSB for three years. He has publis hed over 130 articles on process control and related topics. He is co-author of an award-winning 1989 textbook, *Process Dynamics and Control*, with Profs. Mellichamp (UCSB) and Edgar (University of Texas). He is also co-author of *Multivariable Computer Control—A Case Study* and co-editor of *Chemical Control Process 2.*

Dr. Seborg has received several national awards, which include the 1992 Education Award from the American Automatic Control Council, the Joint Automatic Control Conference Best Paper Award, as well as the Technical Achievement Award from the AIC hE Southern California Section. He is an active industrial consultant and has served as director of three organizations: the American Automatic Control Council, the AIChE Computing and Systems Technology Division, and the ASEE ChE Division. He was general chairman for the 1992 American Control Conference, Chicago, IL. He currently serves on the editorial boards of two journals: *Proceedings of the IEE on Control Theory and Applications* and *Adaptive Control and Signal Processing.*